AD-A031 201 AMERICAN OPTICAL CORP SOUTHBRIDGE MASS F/G 4/1
ERBIUM LIDAR CLOUD BASE MEASURING SYSTEM.(U)
AUG 76 J SEGRE F19628-74-C-0150
UNCLASSIFIED AO-623-F AFGL-TR-76-0177 NL

1 OF 1
AD A031 201

END
DATE FILMED
11-76

AFGL-TR-76-0177

13

B.S.

ERBIUM LIDAR CLOUD BASE MEASURING SYSTEM

By
Joseph Segrè

American Optical Corp.
Southbridge, Mass. 01550

Final Report
1 January 1974 to 1 July 1976

August 1976

Approved for public release; distribution unlimited

Prepared for

Air Force Geophysics Laboratory
Air Force Systems Command
United States Air Force
Bedford, Massachusetts 01731

SECURITY CLASSIFICATION OF THIS PAGE (When Data Entered)

REPORT DOCUMENTATION PAGE

READ INSTRUCTIONS BEFORE COMPLETING FORM

1. REPORT NUMBER: AFGL-TR-76-0177	2. GOVT ACCESSION NO.
3. RECIPIENT'S CATALOG NUMBER	
4. TITLE (and Subtitle): Erbium Lidar Cloud Base Measuring System	5. TYPE OF REPORT & PERIOD COVERED: Final Report. Jan 74 - 74 January-76 July 76,
	6. PERFORMING ORG. REPORT NUMBER: AO-623-F
7. AUTHOR(s): Joseph Segre	8. CONTRACT OR GRANT NUMBER(s): F19628-74-C-0150 New
9. PERFORMING ORGANIZATION NAME AND ADDRESS: American Optical Corp. Southbridge, Mass. 01550	10. PROGRAM ELEMENT, PROJECT, TASK AREA & WORK UNIT NUMBERS: 62101F 66700401
11. CONTROLLING OFFICE NAME AND ADDRESS: Air Force Geophysics Laboratory Hanscom AFB, Massachusetts 01731 Monitor/Eugene Y. Moroz/LYU	12. REPORT DATE: August 1976
	13. NUMBER OF PAGES: 36 (12) 37 p.
14. MONITORING AGENCY NAME & ADDRESS (if different from Controlling Office)	15. SECURITY CLASS. (of this report): Unclassified
	15a. DECLASSIFICATION/DOWNGRADING SCHEDULE

16. DISTRIBUTION STATEMENT (of this Report)
Approved for public release; distribution unlimited.

17. DISTRIBUTION STATEMENT (of the abstract entered in Block 20, if different from Report)

18. SUPPLEMENTARY NOTES
Tech, other

19. KEY WORDS (Continue on reverse side if necessary and identify by block number)
Cloud height measurements, infrared laser, erbium ceilometer, germanium photodiode, single ended, rain, snow, or fog detection.

20. ABSTRACT (Continue on reverse side if necessary and identify by block number)
Results of development and testing of an Erbium Doped Glass Laser Ceilometer are presented and discussed. Various cloud returns, corresponding to differing weather conditions are shown. The Rain, Snow, or Fog Detector is discussed.

DD FORM 1 JAN 73 1473 EDITION OF 1 NOV 65 IS OBSOLETE

SECURITY CLASSIFICATION OF THIS PAGE (When Data Entered)

025 350

CONTENTS

ILLUSTRATIONS

ACKNOWLEDGMENTS

In addition to the author, the team included Mr. Norman Truscott, Mr. John Scully, and Mr. Douglas Waite.

Thanks are due to Mr. Eugene Moroz for his help and interest throughout the project, and for making the necessary arrangements for the tests at AFGL, and to whose personnel we are also indebted. In particular, Mr. George Travers was most helpful in assisting with the AFGL tests.

We gratefully acknowledge the support and continuing technical guidance of Dr. Elias Snitzer, Director of Advanced Research at American Optical.

INTRODUCTION

In the U.S. cloud height has traditionally been obtained with Rotating Beam Ceilometers (RBC's) using a triangulation technique.

When Laser Range-finders, also known as Lidars, were developed it seemed that one of the ideal applications for them would be as cloud height monitoring devices. As a Lidar is a single ended device, the installation and alignment problems that exist with RBC's are virtually eliminated. The measurement accuracy of a Lidar differs from that of an RBC in that is is essentially constant as a function of range, being limited by the pulse length and the bandwidth of the receiving system.

Requirements for Lidars to be used near airports and weather stations are that the device present no hazard to eye safety and that the beam not be visible to the point where it could interfere with a pilot's normal visual tasks. Beam visibility can be overcome by going to the near infrared or the near ultraviolet, but eye safety remains a problem in these regions as most of the available wavelengths still have a high enough transmission in the ocular media to allow for the possibility of retinal damage on direct exposure to a beam. One approach to reduce the eye hazards has been to reduce the peak power in the beam, expand its diameter, and operate at repetition rates of several hundred HZ. Range gating and signal averaging allow processing of return signals with

low signal/noise ratios. This technique, however, has its limitations as the sky background from brightly backlit clouds can reduce the effective range of such a system. Increased range would not then be available without increasing the source brightness, which would make the Lidar less eyesafe.

One of the prime objectives of this program has been to develop a Lidar Ceilometer which is eyesafe and yet exceeds the desired range requirements by a comfortable margin.

The Erbium Doped Glass Laser was developed by American Optical in 1965 for eyesafe Lidar applications. The atmospheric transmission at this wavelength is high, and most optical materials transmit as well here as in the visible and near infrared. The absorption coefficient of water at this wavelength is approximately 90%/mm, making it virtually impossible for radiation incident on the pupil to reach the retina. The absorption coefficient is, however, not as high at 10 microns wavelength where the volume of absorption can be so small as to cause very high skin temperatures to be reached on exposure to the beam, resulting in possible corneal damage. Based on results of eye damage tests on monkeys showing a corneal damage threshold of 23 joules/cm^2, the ANSI Z-136 standards allow a level of 1 joule/cm^2 for a 30 nanosecond Q-switched laser at 1.54 microns.

If we have a Lidar operating at 1.54 microns wavelength with a pulse peak power of 1 megawatt (35 millijoules

in a 35 nanosecond halfwidth pulse) and the beam output diameter of 25mm, the output energy density is .0071 joules/cm^2 which is an ample margin according to ANSI standards.

Having established that such a system meets safety standards, let us consider its potential performance. We assume a detector NEP of 5×10^{-12} $W\sqrt{HZ}$ rms, and a bandwidth of 3 MHZ. The broadband NEP then becomes 8.66×10^{-9} watts. Neglecting atmospheric attenuation and assuming the cloud to behave as a lambertian surface which, however, stretches the return pulse, we assume a reflectance of 2% and a stretching of one order of magnitude in the return pulse. These assumptions are based on our measurements of cloud returns with the Erbium Ceilometer. At the cloud base we therefore have one megawatt incident power, and the equivalent of two kilowatts being reradiated into π steradians. Let us use a ten inch diameter collecting telescope and find the range R for a signal/noise ratio of ten times the rms Noise Effective Power. We then have:

$$2\times10^{3} \left(\frac{.25}{R}\right)^2 \frac{\pi}{4} \cdot \frac{1}{\pi} = 10\ (8.66\times10^{-9})\ \text{Watts} \qquad R \text{ in meters}$$

$$\left(\frac{.25}{R}\right)^2 = 1.732\times10^{-10}$$

$$R = 19\ \text{km.}$$

The above figure neglects atmospheric attenuation.

Recalculating for an atmospheric transmission of 80%/km:

$$2\times10^{3}\left(\frac{.25}{R}\right)^{2}\cdot\frac{1}{4}\,e^{-2\alpha R} = 8.66\times10^{-8}\ \text{watts}$$

where $e^{-2\alpha R}$ represents the round trip attenuation $\alpha = 2.23\times10^{-4}$

$$e^{-2\alpha R}\left(\frac{.25}{R}\right)^{2} = 1.732\times10^{-10}$$

$$\frac{e^{-\alpha R}}{R} = 5.26\times10^{-5}$$

$$R = 5.54\ \text{km.} = 18{,}100\ \text{ft.}$$

The sky background at this wavelength with clouds present is given by Ross[1] as: $P_{SB} = 4\times10^{-4}$ watts/cm^2-ster-micron

For our system: $A = 506\ \text{cm}^2$
$\theta = 2.35\times10^{-7}$ steradians
$\Delta\lambda = 0.6$ microns

And the sky background contribution to the receiver noise would be: 1.36×10^{-13} watts $\sqrt{\text{HZ}}$. Since this is considerably lower than the internal receiver noise, the above range equations are unaffected by sky background conditions.

From the above calculations and the experimental data presented in this report, it can be seen that the major objectives of this program have been met. The system is eyesafe, and has a cloud height range capability well beyond 12,000 ft., the limit of the present range processing and display system.

---

[1] Monte Ross, "Laser Receivers", John Wiley 1966, pp 276-7

DESCRIPTION OF CLOUD HEIGHT MEASURING SYSTEM

The basic system is shown in block diagram form in Fig. 1.

Transmitter Portion

The transmitter has, as the active medium, a 75mm long glass rod having a 4mm core doped with Yb^{3+}, Er^{3+} (the lasing action being due to the $^4I_{11/2} - {}^4I_{13/2}$ transition in the Er^{3+}) and a 6mm o.d. cladding doped with Nd^{3+} and Yb^{3+} as well as other ions used to bring the thermal expansion coefficients of the core and cladding close enough to each other to avoid a highly strained combination on cooling. The Nd^{3+} ion is necessary to improve the pumping efficiency of the laser with broad-band pumping sources. As it also has been found to quench the Er^{3+} fluorescence, the optimum solution was found to be the core-cladding combination in which the Nd^{3+} and Er^{3+} ions are not in the same glass host. The glass rod was coupled to two 75mm long, 4mm bore flashlamps in a semi-imaging system using silver front surface reflectors on quartz. The silver was overcoated to prevent tarnishing. The long fluorescence lifetime of the erbium ion (8-10 milliseconds) and the fact that the pumping bands of the Nd^{3+}, Yb^{3+} ions are principally in the near infrared, allows pumping with a long duration flashlamp pulse at relatively low current densities. The pump pulse is shown in Fig. 2. Input energy is about 250 joules.

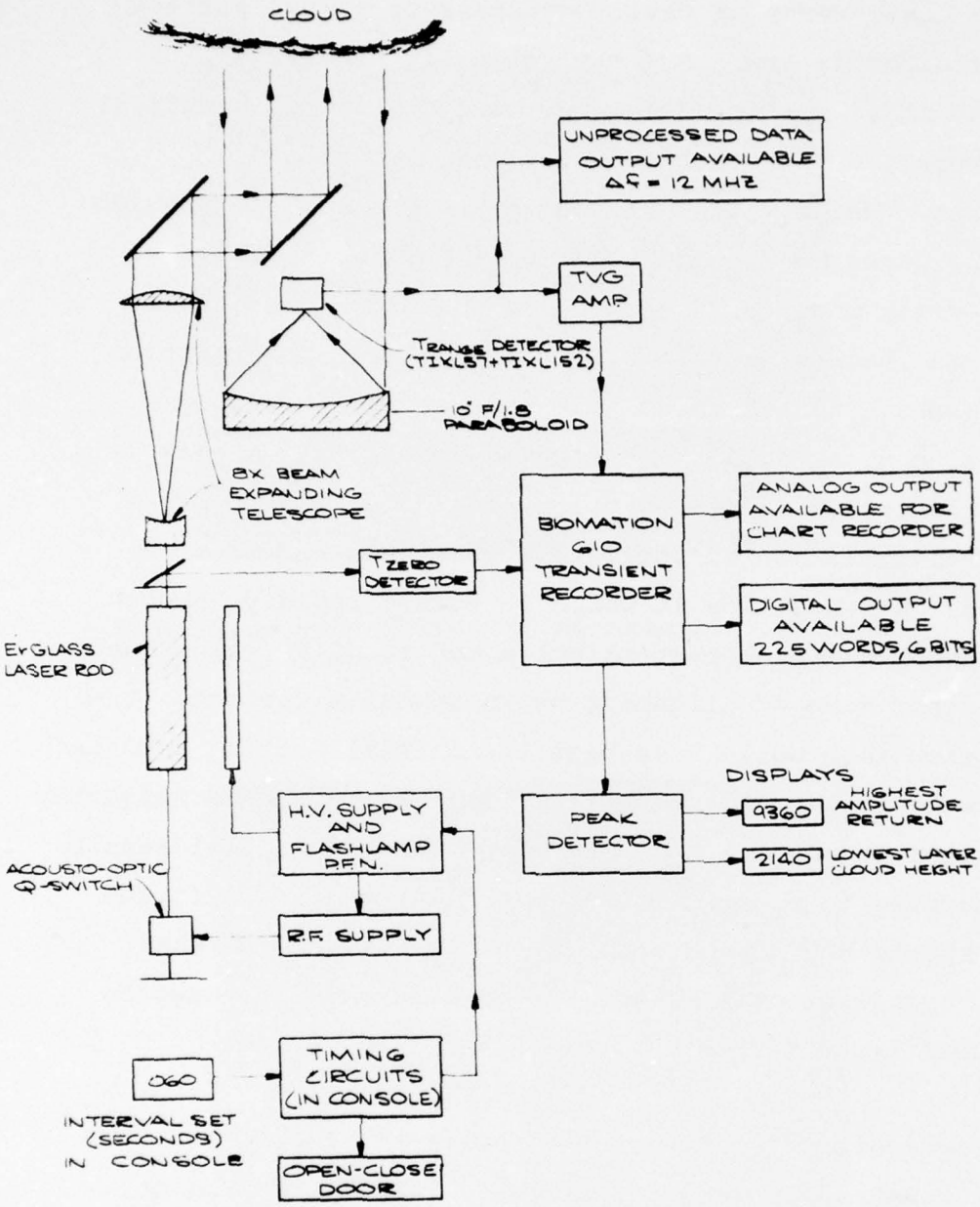

Fig. 1 ERBIUM LASER CEILOMETER BLOCK DIAGRAM

The laser resonant cavity consists of a 100% reflecting rear dichroic and a 60% reflecting front element. The first model Erbium Ceilometer built by American Optical uses a rotating reflector Q-Switch which rotates at 24,000 rpm. While this performed quite well, a unit having no moving parts was considered a more desirable solution. Electro-optic modulators were ruled out because of transmission and damage problems, as well as their polarization requirements. A high speed galvanometer was initially tried as an alternative to the rotating mirror. It was hoped that the galvanometer mirror could be held to one side of alignment until sufficient inversion had been achieved. At that time it would be pulsed rapidly through alignment with a high current pulse and finally, maintained on the other side of alignment by an opposite current. The only motion then would have been the initial setting and the rapid sweep through alignment. A small, light, rear reflector was mounted on the galvanometer shaft and the initial results were encouraging enough to continue this approach. In the end it had to be abandoned, however, because of the shaft wobble which was on the order of the laser beam divergence and caused large variations in the laser output.

Q-Switching by means of a quartz acousto-optic modulator set at the Bragg angle, was finally settled on. The modulator is turned on at the time of flashlamp triggering, and is turned off again about 6 milliseconds later. The turnoff time is extremely rapid, being on the order of 1-2 cycles. A few microseconds after the RF has

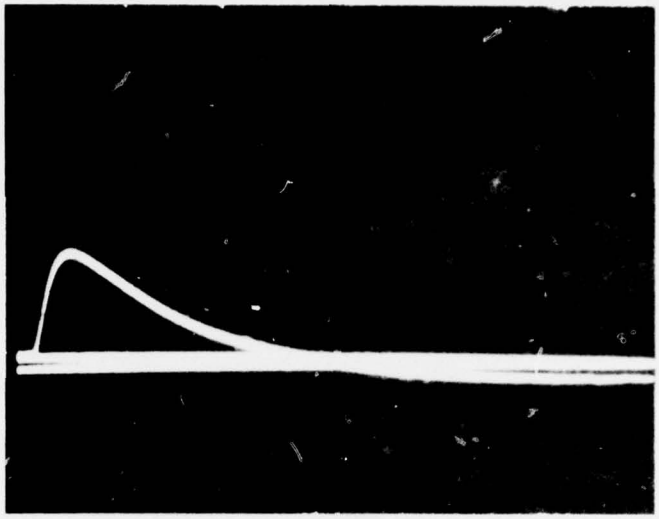

Flashlamp pump pulse. Time base is 2 msec./cm. Q-Switching occurrs 5 msec. after start of pulse.

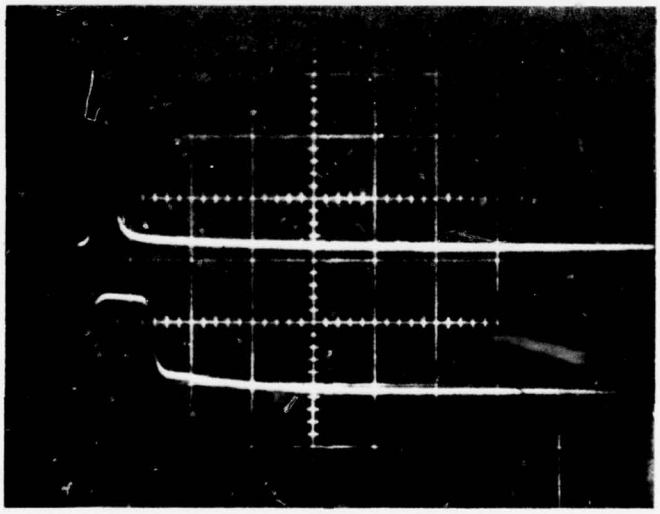

Laser output - 200 nanoseconds/cm. Upper trace is laser output as seen by external detector. Bandwidth is sufficient to resolve pulse. Lower trace is output of T_{zero} detector. Note clipping of signal.

Fig. 2

been turned off, the acoustic field collapses. The resultant Q-Switching action is fast enough to allow a clean 1 megawatt, 35 nanosecond halfwidth pulse to be generated. The output is optimized by varying the RF burst duration. This acts as the Q-Switch variable delay.

An advantage of the acousto-optic modulator is that if desired, the laser can be operated in the long pulse mode by simply turning off the RF supply. This allows testing of the laser efficiency independently of the Q-Switching performance. Because of the above, the acousto-optic modulator appears to be the most desirable solution found to date.

Receiver System

The receiver consists of a germanium photodiode (Texas Instruments TIXL57) at the focus of a 10" diameter F/1.8 aluminized paraboloid. The detector diameter is .25mm, giving a field of view of 0.54 milliradians. It had originally been planned to use this detector in the avalanche mode, but laboratory tests showed that an avalanche gain of 4 was the maximum obtainable before the dark current rose to a level where the overall signal/noise ratio was degraded below that of the non-avalanche mode. In view of the fact that avalanche operation requires a highly stable temperature compensated supply, and that the ceilometer performance was such that a signal/noise ratio of 50:1 was achieved with clouds at 10,000 ft., it was felt that the added complication of operating the detector in the avalanche mode was unnecessary. The

detector is followed by a TIXL152 transimpedance amplifier which gives a bandwidth of 12-18 MHZ for the combination. For unprocessed data examination, a X100 amplifier/line driver combination is used which will drive several hundred feet of BNC cable into an oscilloscope. A similar amplifier/driver combination is used for the T_{zero} signal. With the above bandwidth, most cloud detail revealed by a 35 nanosecond pulse can be observed. This bandwidth is, however, excessive for our processing system. For cloud layer height identification using a peak detector, the cloud return fine structure can contain several inflection points on the return from a single layer if the cloud is not very homogeneous, possibly resulting in spurious readings. The actual bandwidth used is determined by the output characteristics of Biomation 610 Transient Recorder. It is about 2.5 MHZ.

Signal Processing

Range compensation is set for 1/r function, with the Time Variable Gain Amplifier function triggered by the T_{zero} pulse. The output of the Time Variable Gain Amplifier goes directly into the Biomation Transient Recorder, where it is stored in the recirculating memory. This memory has 225, 6 bit words; each word is 100 nanoseconds long, giving us 50 ft. range resolution. The peak detector circuitry processes the recirculating memory output rather than the raw data. The words output at a 2 microsecond rate allowing a factor of 20 reduction in necessary speed for the peak detector circuitry. On the initial output scan, the first peak position is

identified and is then read out as the lowest cloud layer. The next scan is set such that a peak having a higher amplitude than the previous one erases it, and the position of the peak having the highest amplitude appears at the output. This range appears in the other readout.

Rain, Snow, or Fog Detector

An uncoated beam splitter (8% total reflectance) picks off a portion of the output beam. A corresponding detector, essentially identical to the range detector except for the use of a TIXL151 amplifier giving a 50 MHZ receiver bandwidth, is located next to the main receiver detector. The Rain, Snow, or Fog (RSF) Detector is focused 110 ft. from the Lidar. The beam picked off by the beam splitter intersects the detector field of view at its focus. The receiver cross section at that distance (i.e. the detector image) is very closely matched to the transmitter beam diameter. With this tight coupling a raindrop presents a large signal cross section. The output from the RSF receiver goes into a pair of filters, one having a 10 MHZ high pass characteristic, and the other having a 1 MHZ low pass. The filter outputs go to comparators which examine the signal level. If no outputs appear, we assume clear weather. If a signal appears at the low frequency output and none is present at the other output, we assume there is fog overhead. If a very high amplitude signal appears at the high frequency output, we assume snow is present, as a properly oriented snowflake is the equivalent of a highly cooperative target. Whether a low frequency component is also present does not affect the logic, as the

presence of a very high amplitude high frequency signal can only be due to snow. The presence of a lower amplitude high frequency return indicates rain whether or not a low frequency component is also present. A block diagram of the system is shown in Fig. 3.

Display and Control Console (shown Fig. 4)

The console is connected to the Ceilometer by 100 ft. of cable, allowing some latitude in the outdoor placement of the Lidar while maintaining the console indoors. The console controls and features are as follows:

Main Breaker: This controls the power for the entire system.

"Door Open": Opens the receiver/transmitter window cover when in the manual mode.

High Voltage: Allows flashlamp voltage to be shut off in the manual mode of operation. Allows maintenance on the system without dangers of HV present.

Manual or Automatic Operation: When this is set for manual operation, the Ceilometer will operate when the "fire laser" button is activated, provided that the high voltage is on and that the "door open" button has previously been pushed. When the ceilometer is in the automatic mode of operation, the high voltage is on regardless of the high voltage switch setting. The door opens automatically exposing the transceiver window. After the Lidar has fired, the door closes and the cycle begins again.

Timer: This control sets the interval between measurements and can be set from zero to 999 seconds. The actual minimum

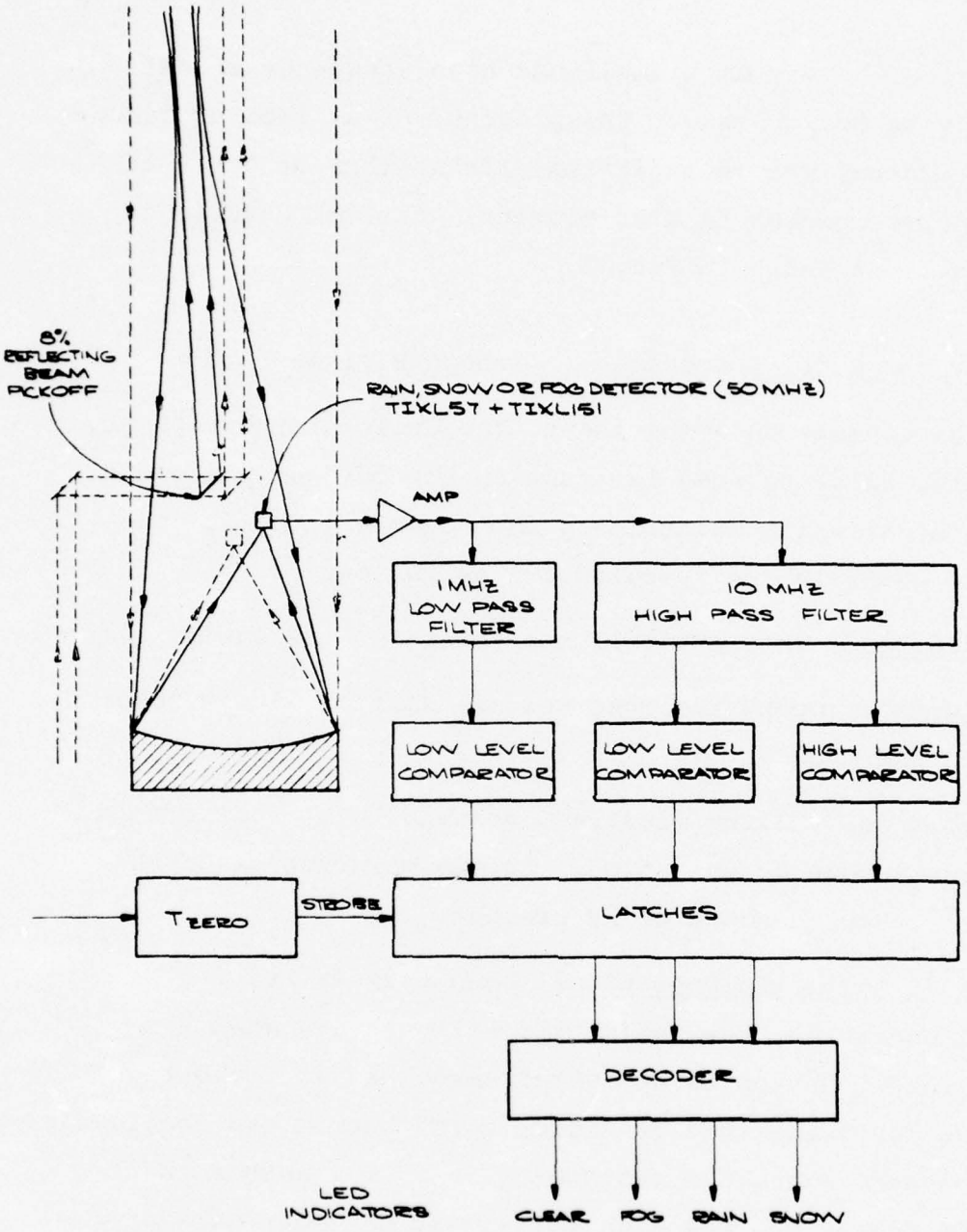

Fig. 3 ERBIUM LASER CEILOMETER
RAIN, SNOW OR FOG DETECTION SYSTEM
BLOCK DIAGRAM

Fig. 4

Erbium Laser Ceilometer Display and Control Console.

interval is set by the laser and the power supply charging time. 60 seconds is the recommended minimum interval.

Displays

Range Display: The Range Display indicates the height of the lowest cloud layer and that of the cloud layer having the highest amplitude return, after the amplitude compensation introduced by the time variable gain function. If only one cloud layer is detected, or if the lowest cloud layer has the highest amplitude, then the range to the lowest cloud will appear in both readouts. If the laser has operated properly and no returns are seen, the display will blink at a frequency of approximately 2 HZ. This indicates that a T_{zero} pulse occurred, the Biomation was triggered, and that the peak detector found no peaks stored in the memory. While the display continues to blink, the data from the previous measurement remains displayed.

Rain, Snow, or Fog Display: Three light emitting diodes (LED) at the base of the control console indicate the presence of rain, snow, or fog as detected by the RSF processing system. If none of the three LED's light, it is assumed that there is clear weather above the ceilometer. Threshold settings for the three indicators are possible with three potentiometers available at the rack front panel, once the sides of the ceilometer housing have been removed.

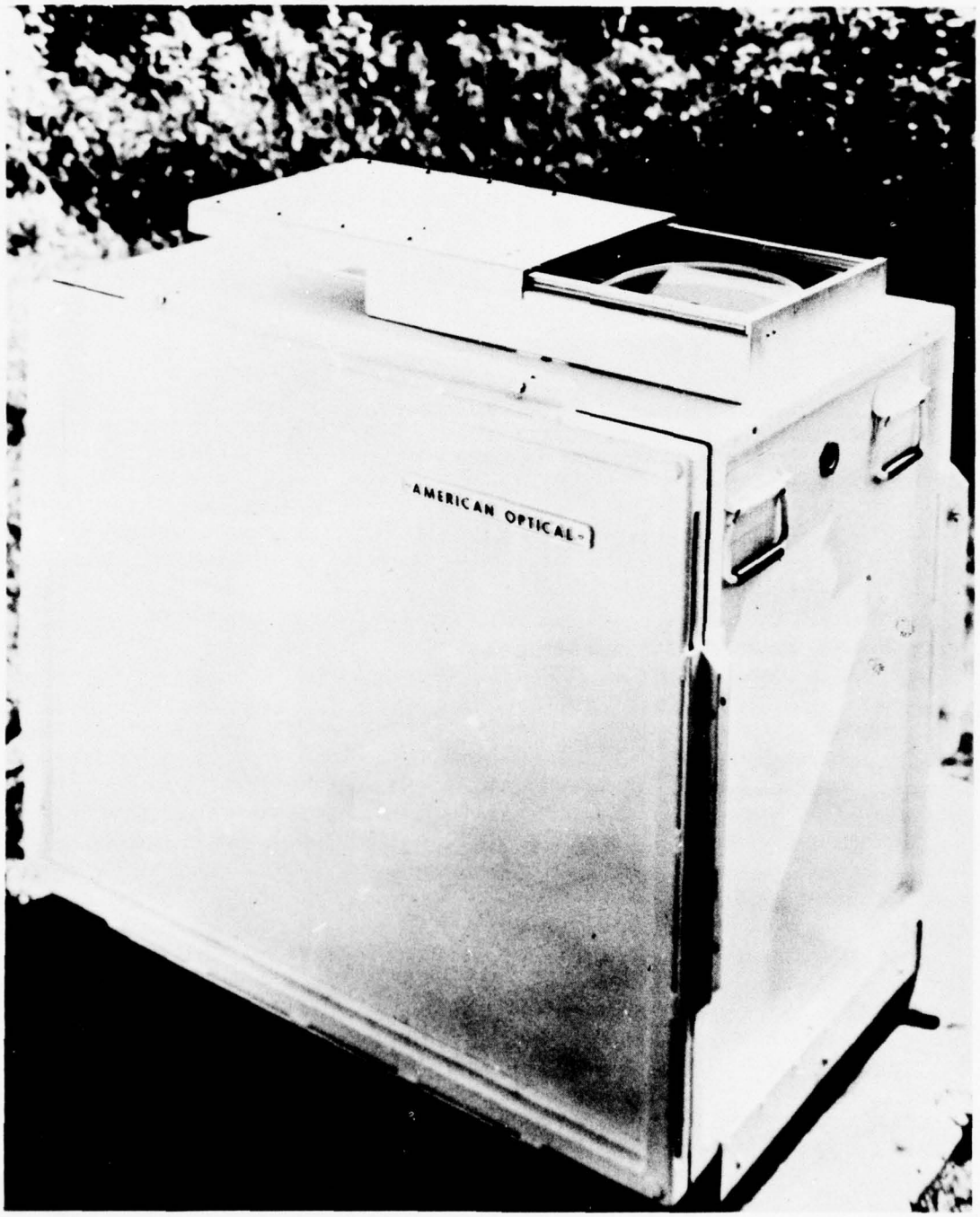

Fig. 5

Erbium Laser Ceilometer Display showing receiver cover open.

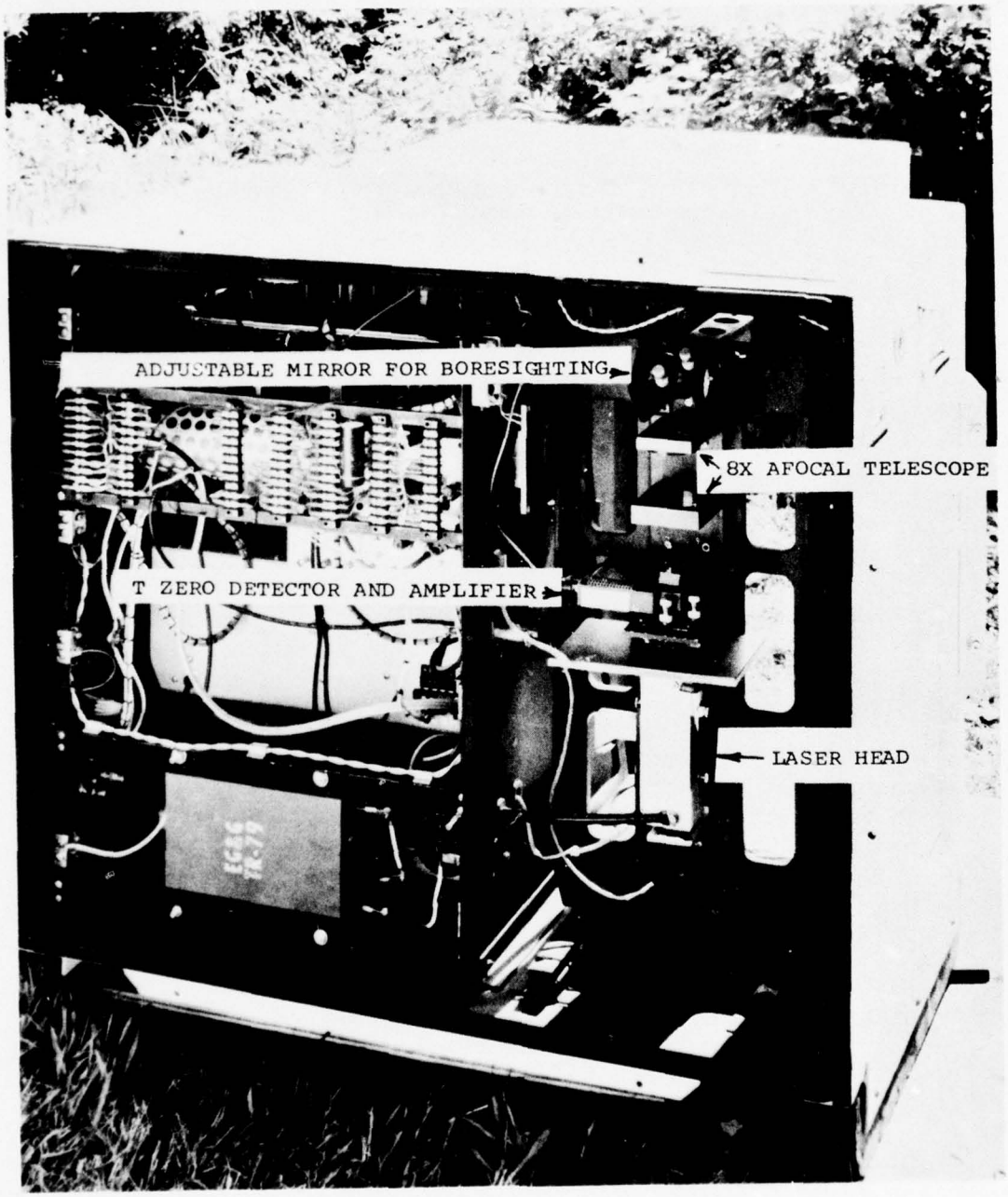

Fig. 6

Erbium Laser Ceilometer Display showing front cover removed.

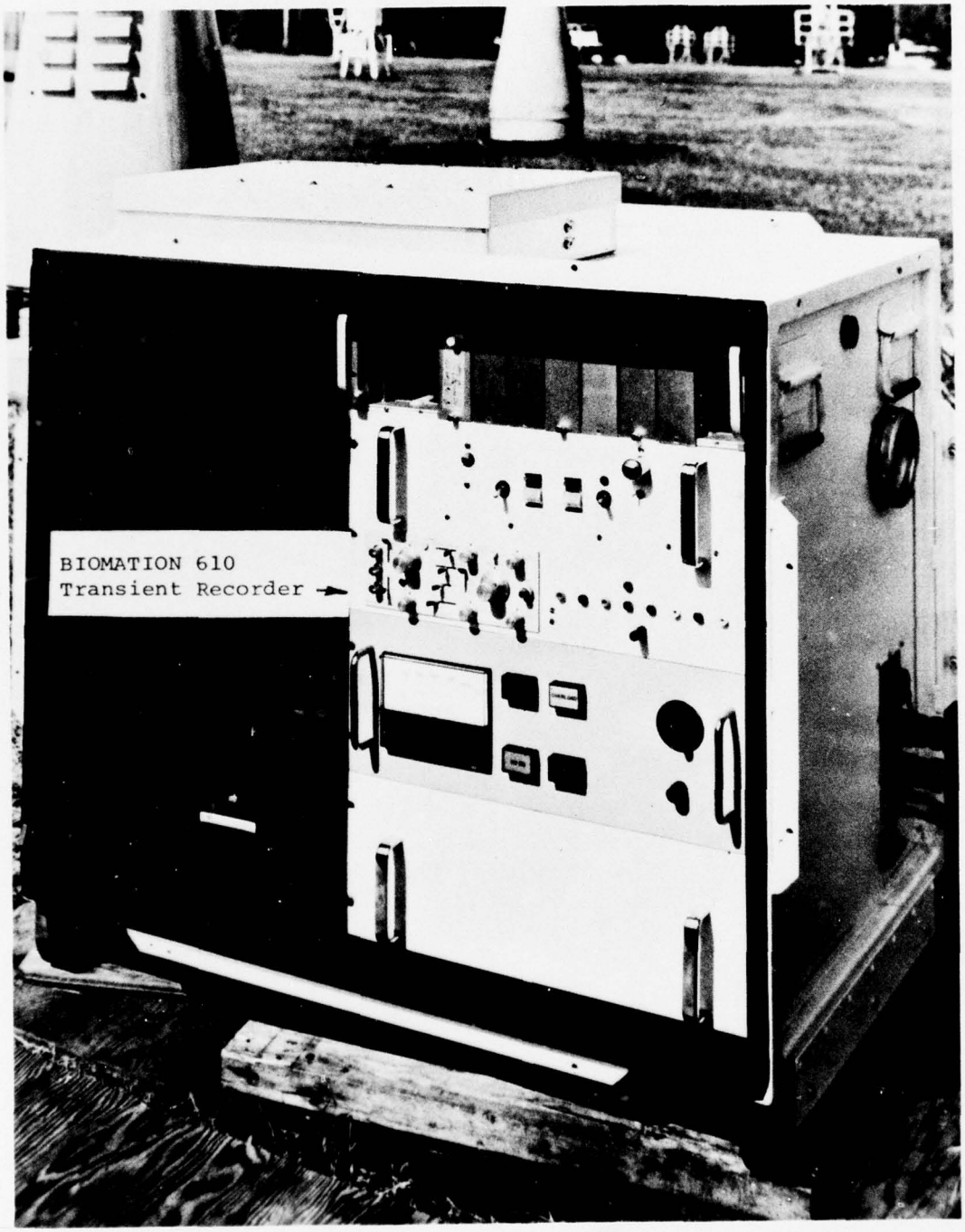

Fig. 7

Erbium Laser Ceilometer Display showing rear cover removed.

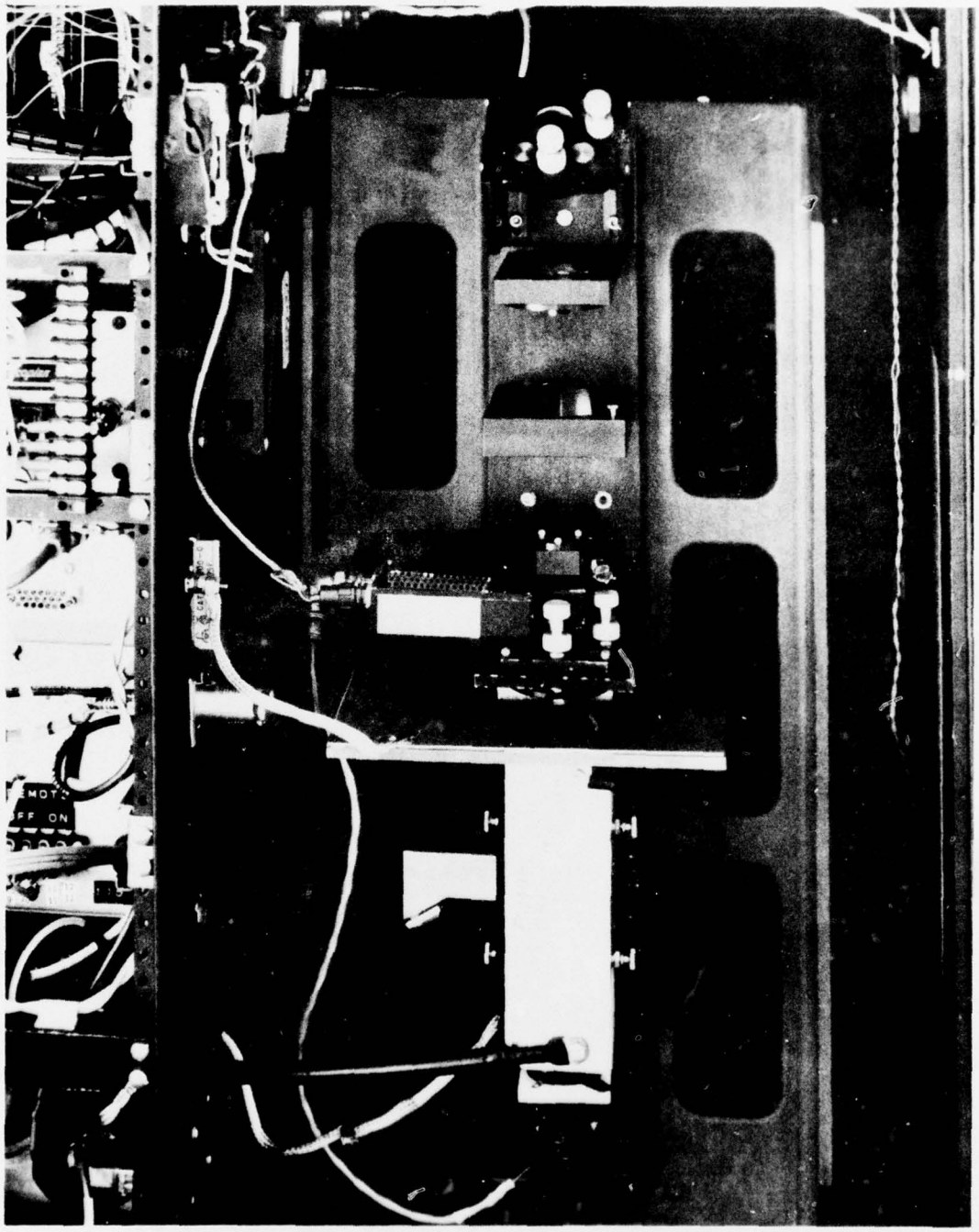

Fig. 8

Closeup of laser head, showing T_{zero} detector and beam expanding afocal telescope.

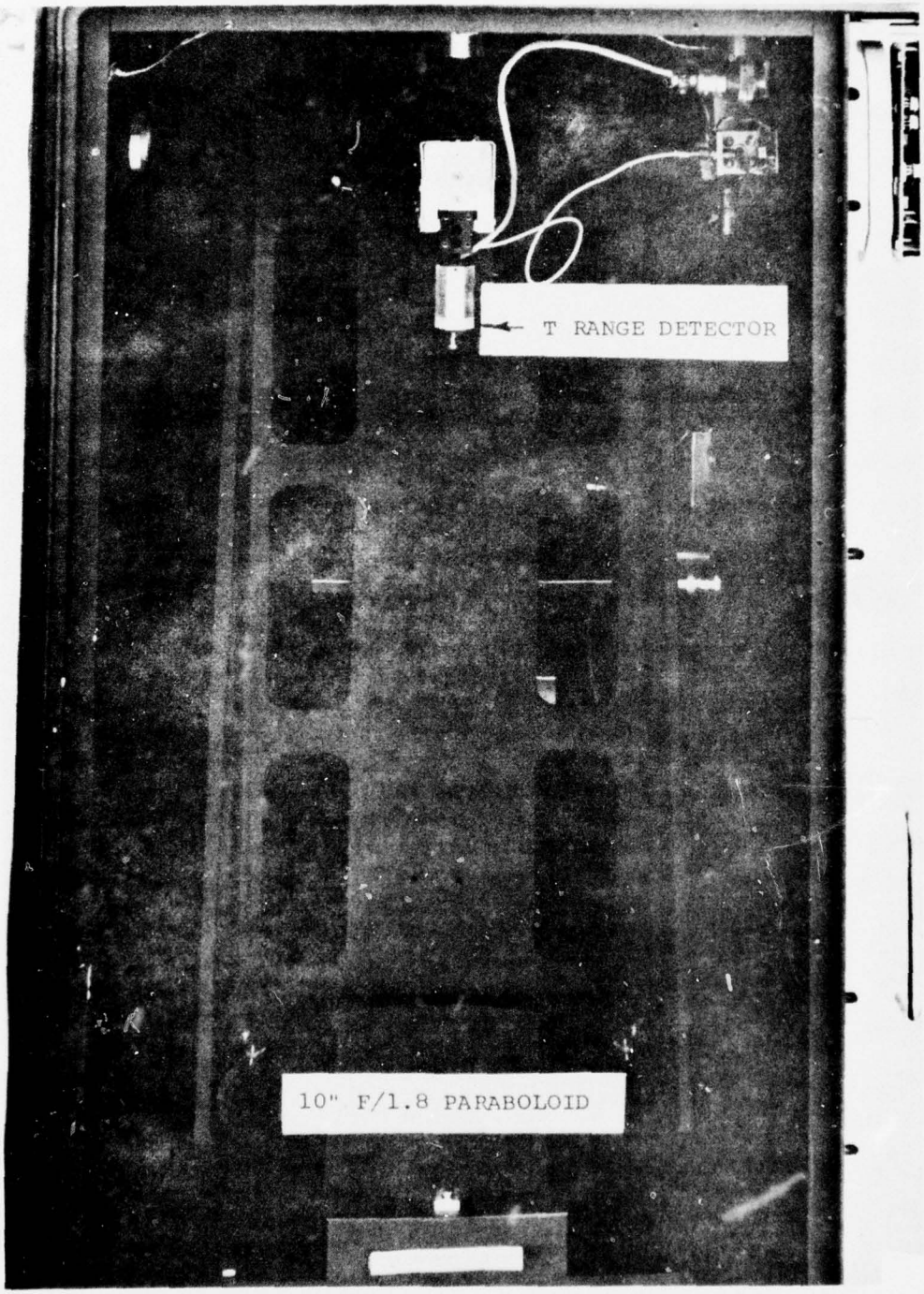

Fig. 9

Receiver, showing T_{range} detector and paraboloid.

RESULTS

Data from four sets of measurements are presented in Fig. 10. If we assume a peak output power of 500 kilowatts and a pulse stretching factor of one order of magnitude, the range curves for clouds having a Lambertian reflectance of 1%, 5%, and 10% are shown superimposed on the data. Considerable variation in cloud reflectance is seen to exist. It is partially accounted for by the varying density of the clouds. Our conclusion from this data was that a $1/r$ time variable gain function was no less valid than a $1/r^2$ function. Due to the increase in dynamic range allowed with the $1/r$ function, this was adopted. This preference can be appreciated by considering that a $1/r^2$ function covers two orders of magnitude dynamic range between 600 ft. and 6,000 ft. With the order of magnitude variation that exists for cloud reflections, the entire receiver dynamic range would be used up over this distance interval.

The effect of atmospheric attenuation does not show up directly from these data. In view of the fit of the data from the cloud bases at 10,000 ft. to the range equation with negligible atmospheric attenuation assumed, we can consider at least 90% atmospheric transmission/km. in clear weather to be a good fit to the existing data.

The receiver field of view is .5 milliradians, matching the laser beam divergence. We have used glass wedges having a .8 milliradian beam deviation in front of the transmitted beam to degrade the system boresighting. As expected, the

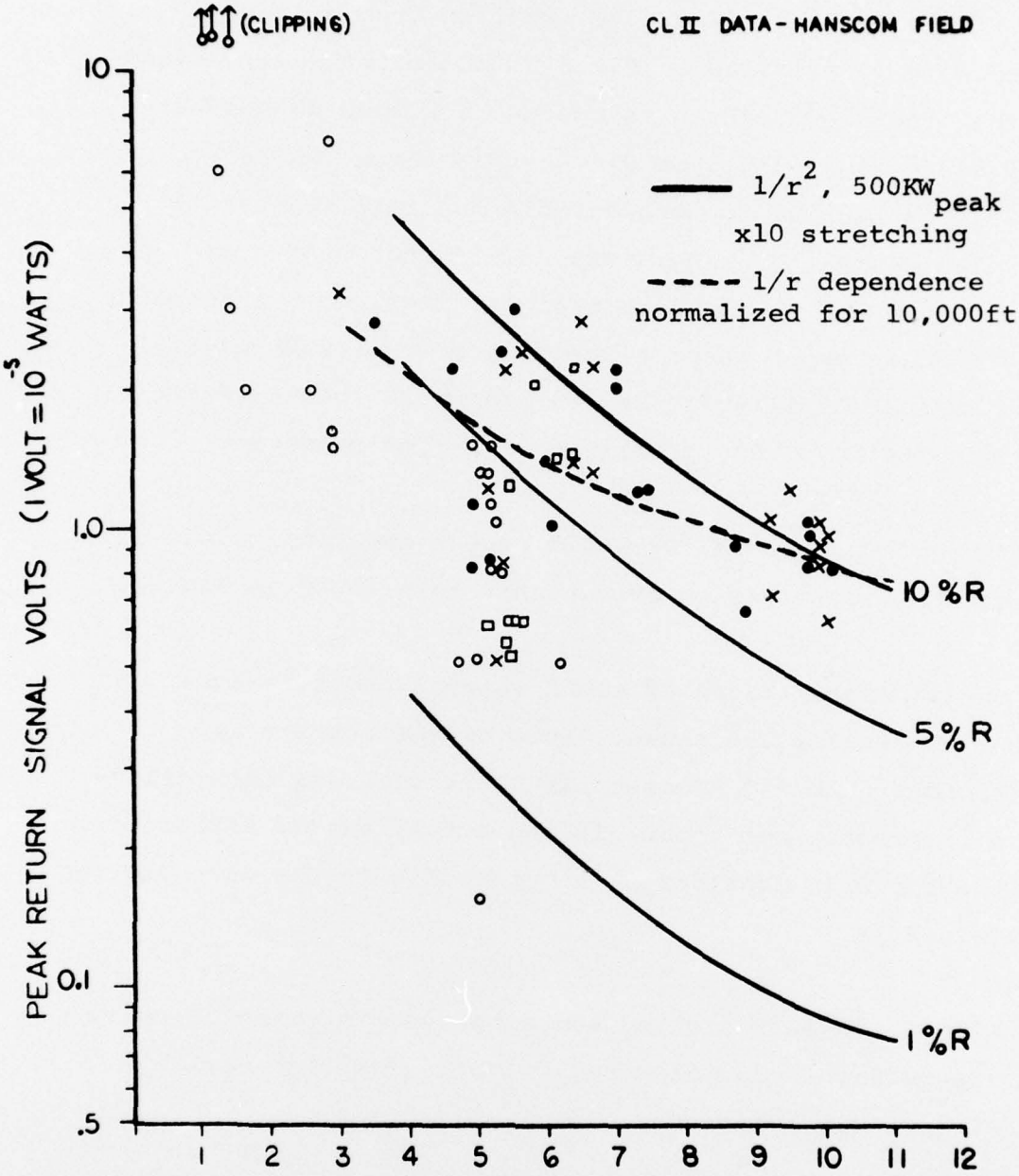
(CLIPPING)
CL II DATA - HANSCOM FIELD
10
1.0
0.1
.5
PEAK RETURN SIGNAL VOLTS (1 VOLT = 10^-5 WATTS)
1/r^2, 500KW peak
x10 stretching
1/r dependence
normalized for 10,000ft
10 %R
5 %R
1 %R
1
2
3
4
5
6
7
8
9
10
11
12
RANGE — THOUSANDS OF FEET

Fig. 10

return signal from clouds was attenuated. The degradation, however, was less than would be expected from a source subtending a .5 milliradian field at the cloud base, indicating that the cloud return is coming back from a somewhat larger source than the beam diameter at the cloud base. This is probably due to considerable multiple scattering and indicates that we should expect a factor of two or three improvement in the return signal level with a detector having a diameter at least twice that of the .25mm of the Texas Instruments TIXL57. We are presently investigating the tradeoffs involved in going to a larger detector.

Based on the above, we would expect the final cloud reflectance figures to be even higher than shown in Fig. 10.

Oscilloscope traces of cloud returns under various weather conditions are shown. Some of the returns are much broader than 350 nanoseconds halfwidth, and accordingly, have a lower peak amplitude. If the actual energy reflected from the cloud is considered, a better fit to the data plotted is obtained.

All of the data plotted and displayed is taken directly from the detector amplifier and driver. The time variable gain circuit was bypassed.

The readout display was able to pick out the return pulse with the highest amplitude consistently and display its height in the appropriate readout. If there were no cloud returns within the 12,000 ft. range of the processing system, the display went into the "blink" mode as designed.

The Rain, Snow, or Fog Detector has been tested with simulated signal and found to function as designed. Tests are continuing with both real and simulated weather conditions in order to optimize the system calibration. The RSF transmitter power output is 8% of the primary beam. Unlike the main system, the RSF system does not have a coaxial configuration. The transmitter and receiver axes are not parallel, but intersect at some height above the instrument. The receiver detector is not focused at infinity but, rather, for the height of intersection with the transmitter beam. At present, the distance chosen is 110 ft. Both the transmitter beam cross section and the receiver detector image are about one inch in diameter at that distance. This geometry yields very strong coupling for rain drops that happen to occupy that particular common volume at the time of measurement. But the probability of having a sufficient number of drops in that volume may be too low for consistent rain readings. By moving the point of intersection out, the detector image size at that point increases and the common volume is, therefore, correspondingly increased. The result is that while the optical coupling for a given drop decreases with distance, the number of drops within the volume would be expected to increase. Further measurements should help to determine the optimum intersection distance. It will also be possible to increase the reflectance of the transmitter beam pickoff as the main system range capabilities appear to exceed stated requirements under most conditions.

Cloud layer
at 16,500 ft.

8,750 ft. layer
appearing,
higher layer
return barely
detectable

Lower layer
has thickened,
upper layer
return is lost

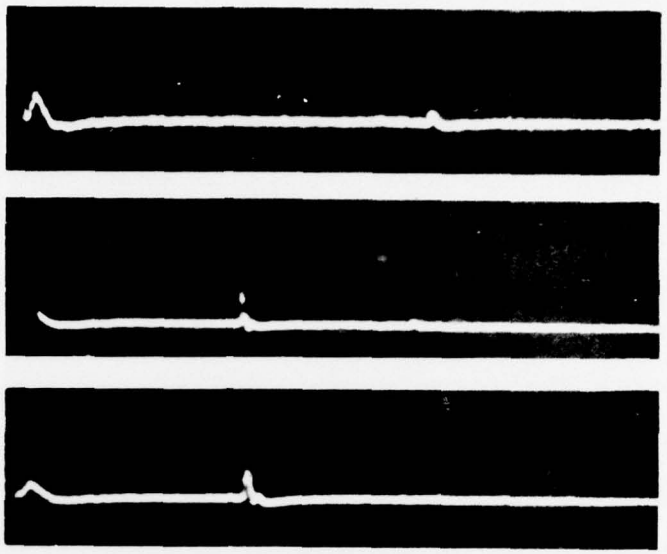

5 μ sec/div. 0.5v/div.
Data showing return from cloud layers at
16,500 ft. and 8,750 ft.

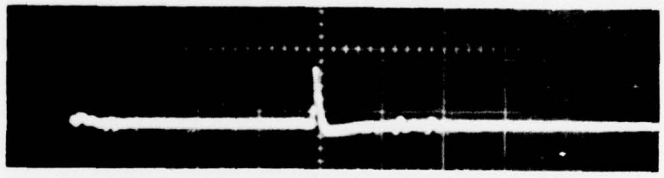

5 μ sec/div. 1 v/div.
Solid cloud layer, clear weather below.
10,000 ft. readout.

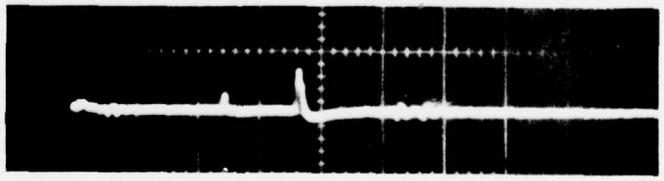

5 μ sec/div. 1 v/div.
Appearance of lower layer at 6,000 ft.
Upper layer readout 9,250 ft.

Fig. 11

All traces 2 μ sec/div. 1 v/div.

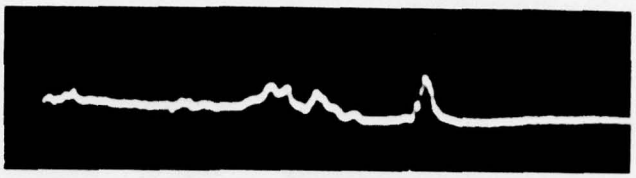

Note extended cloud return from 3,000 ft. to 5,000 ft. with highest amplitude return from layer at 6,100 ft.

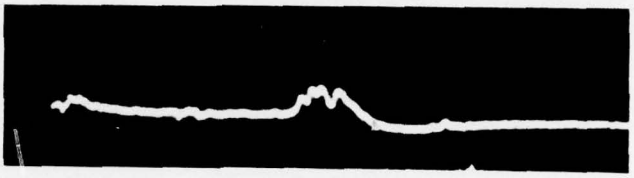

Here, extended return is now higher and upper layer return is almost lost.

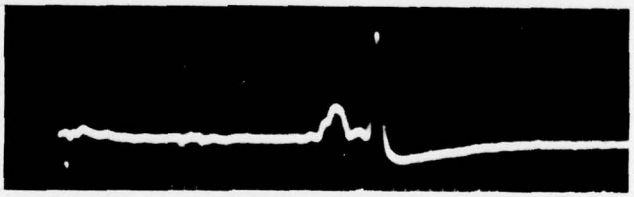

Here, layer at 4,400 ft. is more distinct, with solid layer appearing at 5,000 ft.

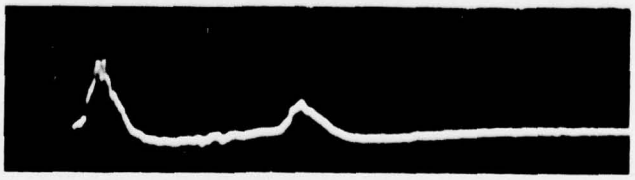

Main return is at 3,600 ft. Note high amplitude of near-in return.

Fig. 12

Rain returns. 1 μ sec/div. 05 v/div.

1 μ sec/div. 1 v/div.
Note extended return ending in base of solid layer at 2,900 ft. in upper trace, while lower trace has principal layer at 2,700 ft. emerging from middle of extended return.

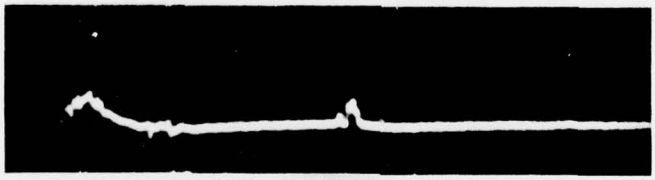

Heavy rain with very large drops. Layer at 4,600 ft. 2 μ sec/div. 1 v/div.

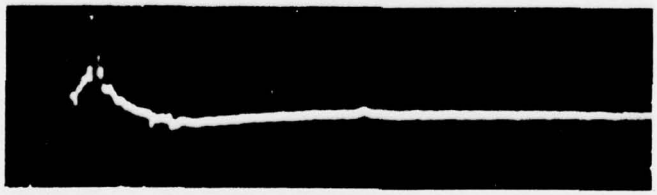

Note increase of rain return. 4,600 ft. layer barely detectable. 2 μ sec/div. 1 v/div.

Fig. 13

Showing detail of near-in return. Spikes are large raindrops. Note amplitude of near-in return extends above baseline to 1,800 ft. range. 2 μ sec/div. 0.5 v/div.

Fig. 13

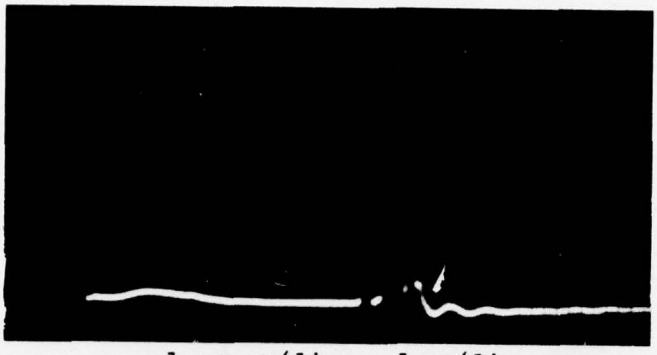

1 μ sec/div. 1 v/div.
Lowest layer is at 2,500 ft. Amplifier saturation occurs for layer at 3,000 ft. Third layer is at 3,200 ft.

2 μ sec/div. 1 v/div.
Main return at 900 ft., second layer at 1,250 ft., second highest amplitude return at 1,500 ft., fourth layer is at 2,050 ft.

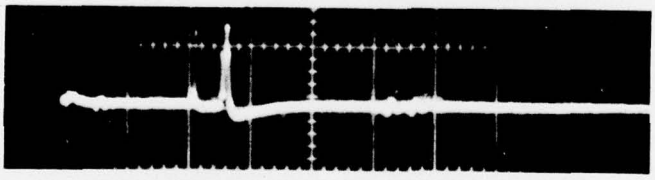

5 μ sec/div. 1 v/div.
Layers at 5,200 ft. and 6,650 ft. Second layer has a slightly higher return amplitude.

Multilayer Returns Fig. 14

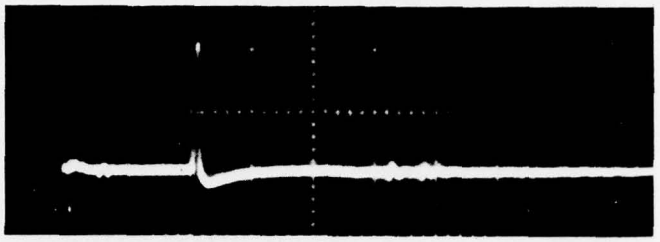

5,400 ft. readout

5 μ sec/div. 1 v/div

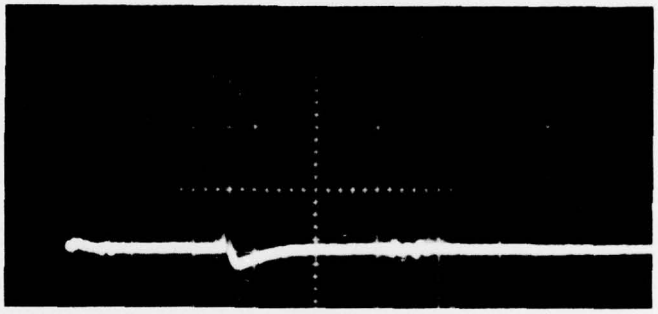

6,500 ft. readout

5 μ sec/div. 1 v/div.

Typical Single Layer Returns Fig. 15

CONCLUSIONS

The Erbium Lidar Ceilometer has met the desired criteria for a cloud base height measuring system. The device is eyesafe, invisible to the eye, and has sufficient range capability to measure cloud heights up to more than 12,000 ft. The processing electronics has a resolution of $\pm$50 ft. and readings have been observed to stay within this limit for stable cloud layers. When the cloud layer having the highest return amplitude was not the lowest layer, it was correctly designated on the display, as was the lowest layer. When there were no cloud returns, the display went into the "blink" mode as designed.

The Rain, Snow, for Fog Detector appears to work as designed. Further tests will have to be carried out to determine its reliability as an indicator of these weather conditions.

Further experiments will be conducted and additional data taken at AFGL and Otis AFB in the future.

Printed by
United States Air Force
Hanscom AFB, Mass. 01731